The Impact of Rapid Wind Variability upon Air-Sea Thermal Coupling

Philip Sura and Matthew Newman

CIRES Climate Diagnostics Center, University of Colorado
and
NOAA Earth System Research Laboratory
Boulder, Colorado

May 15, 2007

Journal of Climate (in press)

Corresponding author address:
Philip Sura
NOAA-ESRL and CIRES Climate Diagnostics Center, R/PSD1
325 Broadway, Boulder, CO 80305-3328
Phone: (303) 497-4426, Fax: (303) 497-6449
E-Mail: Philip.Sura@noaa.gov

Abstract

The basic effect of extratropical atmosphere-ocean thermal coupling is to enhance the variance of both anomalous sea surface temperatures (SST) and air temperatures (AIRT) due to a decreased energy flux between the atmosphere and ocean, called reduced thermal damping. In this paper it is shown that rapidly varying surface winds, through their influence upon the turbulent surface heat fluxes that drive this coupling, act to effectively weaken the coupling and thus partially counteract the reduced thermal damping. In effect, rapid fluctuations in wind speed somewhat insulate the atmosphere and ocean from each other.

The nonlinear relationship between the rapidly-varying wind speed anomalies and SST and AIRT anomalies results in a rapidly varying component of the surface heat fluxes. The clear separation between the dynamical timescales of the ocean and atmosphere allows this rapidly varying flux to be simply approximated by a stochastic process in which rapidly varying wind speed is represented as Gaussian white-noise whose amplitude is modulated by the more slowly-evolving thermal anomalies. Such state-dependent (multiplicative) noise can alter the dynamics of atmosphere-ocean coupling because it induces an additional heat flux term, the noise-induced drift, that effectively acts to weaken both coupling and dissipation. Another key implication of the outlined theory is that air-sea coupling includes both deterministic and stochastic components.

The theory is tested by examining daily observations during extended winter (November-April) at several Ocean Weather Stations (OWSs). Two important results are found. First, multiplicative noise at OWS P effectively decreases the coupling by about one third, with

about a 10% (20%) decrease in the damping of SST (AIRT). This suggests that multiplicative noise may be responsible for roughly half of the AIRT variability at OWS P on subseasonal timescales. Second, OWS observations reveal that joint probability distribution functions (PDFs) of daily averaged SST and AIRT anomalies are significantly non-Gaussian. It is shown that treating the rapidly-varying boundary-layer heat fluxes as state-dependent noise can reproduce this observed non-Gaussianity. It is concluded that the effect of state-dependent noise is crucial to understand and model atmosphere-ocean coupling.

1 Introduction

Coupling of the atmosphere and ocean is largely due to fluxes of momentum and heat through their common boundary, the sea surface. Most of this exchange is a result of the turbulent nature of the atmospheric boundary layer; molecular momentum and heat transfers play a very minor role in atmosphere-ocean coupling. That is, in an hypothetical world without any sea surface winds there would be little air-sea interaction. Wind-driven turbulent heat fluxes are commonly expressed in terms of simple bulk formulae that depend upon the strength of the wind speed $|\mathbf{U}|$ and typically take the form $f = \beta(T_o - T_a)|\mathbf{U}|$ (positive flux upward), where T_o and T_a are the sea surface temperatures (SST) and air temperatures (AIRT) respectively, and β is a (in general not constant) parameter including the densities of sea-water and air, specific heats, the Bowen ratio, and also other time varying physical processes [see Frankignoul and Hasselmann (1977), Sura et al. (2006) or any textbook on air-sea interaction, e.g. Kraus and Businger (1994), for details]. Variations in this flux can then drive variations in midlatitude SST and AIRT.

Barsugli and Battisti (1998) (hereafter BB98) proposed a simple heuristic model to gauge the effect of atmosphere-ocean thermal coupling, consisting of two linear equations for the rate of change of the AIRT anomaly T'_a and the SST anomaly T'_o:

$$\begin{aligned} \frac{dT'_a}{dt} &= -aT'_a + bT'_o + \eta_a \ , \\ \frac{dT'_o}{dt} &= cT'_a - dT'_o \ , \end{aligned} \tag{1}$$

where η_a is Gaussian white-noise representing rapidly varying weather fluctuations, the parameters a and d are the damping coefficients, and b and c are coupling coefficients. How

surface winds drive surface fluxes was not explicitly considered in this model; rather, BB98 suggest that the coupling coefficients represent the effects of both feedback due to surface fluxes (turbulent and radiative) and the dynamical response of the atmosphere to SST anomalies. The main point of BB98 is that the atmosphere-ocean coupling enhances the variance in both media due to a decreased energy flux between the atmosphere and the ocean, which they termed reduced thermal damping.

BB98 can be viewed as a straightforward extension of the Frankignoul and Hasselmann (1977) null hypothesis for SST variability, where the effect of atmospheric forcing on SST anomalies is commonly represented by a simple stochastic model of the oceanic mixed-layer,

$$\frac{dT_o'}{dt} = -\lambda T_o' + \eta \ , \tag{2}$$

(Hasselmann 1976; Frankignoul and Hasselmann 1977, hereafter FH77). Here, λ is a constant rate coefficient representing the transfer of heat from the slowly evolving mixed-layer heat anomaly and η is Gaussian white-noise representing heat fluxes due to rapidly varying weather fluctuations. However, Sura et al. (2006) (hereafter SNA) showed that this implicitly ignores the effect of rapid variations in the wind speed, $|\mathbf{U}|'$, upon λ. That is, because surface wind speeds have relatively large variability and are almost uncorrelated from day to day, it is more appropriate (as derived from first principles) to parameterize λ as a stochastic process in which $\lambda = \overline{\lambda} + \lambda'$, where $\overline{\lambda}$ is constant but λ' is white noise. This results in the addition of a state-dependent, or multiplicative, noise $-\lambda' T_o'$ to (2) that depends upon the SST anomaly itself. As described in SNA, such multiplicative noise has two notable consequences. First, it results in non-Gaussian probability distribution functions (PDFs) for SSTs, even though the deterministic portion of (2) remains linear. Second, it increases the autocorrela-

tion time scale of SST anomalies, even as the autocorrelation function remains exponential as suggested by FH77. This is a consequence of a phenomenon known as noise-induced drift, which occurs because the time mean of the multiplicative noise term, $\overline{\lambda' T'_o}$, is not zero even though the time mean of λ' is zero. SNA showed that their simple modification of the FH77 paradigm compared well to observed non-Gaussian PDFs of daily SSTs at several Ocean Weather Stations (OWSs), and using a single-column mixed-layer ocean model suggested that most of the multiplicative noise during the cold season (i.e., November-April) was likely due to rapidly varying sensible and latent heat flux anomalies.

The success of the SNA multiplicative noise approach for uncoupled SST variability immediately suggests that it is also relevant to the coupled problem, particularly as formulated by BB98. For example, note that anomalies of the heat flux f can be partitioned into three terms that depend upon the products $|\overline{\mathbf{U}}|(T'_o - T'_a)$, $|\mathbf{U}|'(\overline{T_o} - \overline{T_a})$, and $|\mathbf{U}|'(T'_o - T'_a)$, respectively. While the first term represents deterministic coupling of AIRT and SST anomalies, and the second term is a source of additive (that is, state-independent) noise, the third term potentially represents multiplicative noise. Thus, we might expect that in the BB98 model, the damping and coupling coefficients (a, b, c, d) should all contain stochastic components. As in SNA, noise-induced drift due to fluctuations in the damping coefficients would act to increase persistence of both SST and AIRT anomalies. However, as noted in a different climate context by Sardeshmukh et al. (2001), noise-induced drift due to fluctuations in the coupling coefficients might act to *decrease* persistence, acting to oppose reduced thermal damping. Moreover, stochastic fluctuations in the coupling parameters raises the possibility that not all air-sea coupling is necessarily deterministic, as is assumed in the BB98 framework.

In this paper we study the impact of rapidly-varying (on daily and sub-daily timescales) sea surface heat fluxes on atmosphere-ocean coupling by deriving a simple coupled model of SST and AIRT variability that accounts for rapid fluctuations in surface heat fluxes due to rapid variability of sea surface winds. We restrict our study to the northern hemisphere cold season because then the SST anomaly tendency is predominantly due to the net turbulent heat flux anomalies and not to changes in the mixed-layer depth; also, radiative flux anomalies have only a minor impact during the cold season (Park et al. 2005). The outline of the paper is as follows. First, because noise-induced drift is a critical component of the effect of rapidly fluctuating winds on atmosphere-ocean coupling, we will explain the physical cause of the noise-induced drift in a heuristic way (section 2). The coupled model, similar in form to BB98 except that it includes multiplicative noise, is then introduced in section 3. In section 4 we use inverse methods to estimate the parameters of our simple coupled model, show that the non-Gaussianity of anomalous SST variability during the extended winter season at several Ocean Weather Stations can be reproduced by this model, and discuss the impact of the multiplicative noise on the power spectra of SST and AIRT. Finally, section 5 provides a summary and discussion.

2 Noise-induced drift

To understand how multiplicative noise affects atmosphere-ocean coupling, it is useful to first clarify how introducing stochastic components with zero mean to the coefficients in (1) can nevertheless result in a noise-induced drift. Readers already familiar with stochastic

differential equations may wish to skip this section, whereas those interested in rigorous math should consult one of the available textbooks (e.g., Gardiner 2004; Horsthemke and Léfèver 1984; Kloeden and Platen 1992; Paul and Baschnagel 1999). However, to heuristically explain the noise-induced drift consider the simplified system

$$\frac{d\delta T}{dt} = -\delta T(\overline{|\mathbf{U}|} + |\mathbf{U}|'), \tag{3}$$

where wind-driven heat flux acts to relax (damp) the air-sea temperature difference $\delta T \equiv (T'_a - T'_o)$ towards its climatological (equilibrium) state $\delta T = 0$. The relaxation is forced by two components of the heat flux, one driven by the mean wind speed $\overline{|\mathbf{U}|}$ and the other driven by the anomalous wind speed $|\mathbf{U}|'$.

For some climate problems of interest, stochastic differential equations are obtained by approximating rapidly varying quantities as white-noise. In (3), for example, note that δT evolves much more slowly than $|\mathbf{U}|'$, so $|\mathbf{U}|'$ is approximated by white-noise. In reality, of course, the underlying systems are usually continuous in both time and space. That is, physical processes are often smooth with at least a small degree of autocorrelation. In our specific example this means that there exists a small time increment during which the anomalous wind $|\mathbf{U}|'$ can be considered constant (loosely speaking, this is the definition of a Stratonovich system; see the appendix for a more detailed discussion).

Consider an ensemble of realizations for which it is assumed that the wind anomaly forcing is Gaussian with a standard deviation $\sigma_{|\mathbf{U}|'}$ and PDF $p(|\mathbf{U}|') \equiv p$. We ask how the ensemble mean trajectory that passes through the point δT_0 evolves for a small time increment where the wind speed anomaly $|\mathbf{U}|'$ is approximately constant. To answer, note

that the average response to positive $+|\mathbf{U}|'$ and negative $-|\mathbf{U}|'$ kicks is

$$\langle \delta T_+ \rangle = \delta T_0 \int_0^\infty \exp\left(-(\overline{|\mathbf{U}|} + |\mathbf{U}|')t\right) p\, d|\mathbf{U}|' \quad , \tag{4}$$

$$\langle \delta T_- \rangle = \delta T_0 \int_0^\infty \exp\left(-(\overline{|\mathbf{U}|} - |\mathbf{U}|')t\right) p\, d|\mathbf{U}|' \quad . \tag{5}$$

Therefore, the mean response to the anomalous wind forcing will be

$$\langle \delta T \rangle = \delta T_0 \frac{1}{2} \int_0^\infty \left[\exp\left(-(\overline{|\mathbf{U}|} + |\mathbf{U}|')t\right) + \exp\left(-(\overline{|\mathbf{U}|} - |\mathbf{U}|')t\right)\right] p\, d|\mathbf{U}|' \quad , \tag{6}$$

or

$$\langle \delta T \rangle = \delta T_0 \exp\left(-\overline{|\mathbf{U}|}t\right) \int_0^\infty \cosh\left(-|\mathbf{U}|'t\right) p\, d|\mathbf{U}|' \quad . \tag{7}$$

However, without wind forcing anomalies $\langle \delta T \rangle$ evolves according to

$$\langle \delta T \rangle = \delta T_0 \exp\left(-\overline{|\mathbf{U}|}t\right) \quad . \tag{8}$$

The key point here is that in the presence of anomalous wind speeds $|\mathbf{U}|'$ the average response $\langle \delta T \rangle$ differs from the corresponding response without the anomalous forcing. This occurs due to the physics of the system: weaker wind means weaker heat flux, so that the exponential decay of the air-sea temperature difference is much less rapid in response to a negative wind speed anomaly $-|\mathbf{U}|'$ but only somewhat more rapid in response to an equal amplitude but positive wind speed anomaly $+|\mathbf{U}|'$. That is, the effects of equal but opposite wind anomalies do not cancel each other, resulting in a noise-induced drift of the ensemble mean.

This situation is depicted in Fig. 1, a comparison of (7) (response with anomalous wind speeds; solid line) and (8) (response without anomalous wind speeds; dashed line), for $\overline{|\mathbf{U}|} \equiv 1$, $\sigma_{|\mathbf{U}|'} \equiv 0.5$, and $\delta T_o \equiv 1$. Inclusion of anomalous wind speeds makes $\langle \delta T \rangle$ decay slower

than when there is no wind variability. That is, in this particular case (linear system with linear multiplicative noise) the stochastic forcing effectively reduces the damping of the system. In more general terms, the stochastic forcing induces an additional drift term, the noise-induced drift. Note that this drift, although due to a stochastic (i.e., unpredictable) term, results in a predictable change to the evolution of $\langle \delta T \rangle$.

Finally, let us define the terminology used in the remaining sections (and, in general, in the literature). The mean response of the stochastic system with multiplicative noise [Eqs. (6) or (7) and solid line in Fig. 1] is called the *effective drift*. The mean response of the stochastic system without multiplicative noise [Eq. (8) and dashed line in Fig. 1] is referred to as the *deterministic drift* (or just the *drift*). The difference, that is the mean drift induced by the multiplicative noise, is called the *noise-induced drift*. To summarize: *effective drift* = *(deterministic) drift* + *noise-induced drift*.

3 A Simple coupled model

In this section we show how important rapid surface wind variability is to atmosphere-ocean coupling, and how its effects can be modeled with multiplicative noise. Our approach is to extend the BB98 stochastic model by explicitly considering wind induced heat flux anomalies in the context of a simple mixed-layer model. Recall that BB98 assumed that the coupling coefficient b in their model included the dynamical atmospheric response to SST anomalies. In the following model derivation, coupling is only due to surface heat flux, so all model parameters are based on local coupling alone. However, in section 4 model

parameters will be determined from observations and so might also implicitly include the effects of atmospheric dynamics.

3.1 The basic equations

Consider a one-dimensional thermodynamic model for the upper mixed-layer ocean coupled to a one-dimensional mixed-layer atmosphere. The atmosphere is assumed to be a well mixed and horizontally homogeneous layer with temperature T_a and effective heat capacity γ_a in contact with the underlying ocean, a well mixed and horizontally homogeneous layer of constant depth with temperature T_o and effective heat capacity γ_o. For the sake of simplicity, all effects of horizontal advection, humidity, and salinity are ignored. Then local heat budget equations for AIRT T_a and SST T_o can be written as

$$\gamma_a \frac{dT_a}{dt} = f(T_a, T_o, |\mathbf{U}|) - \lambda_a(T_a - T_{a_e}) + \xi_a \equiv F_a(T_a, T_o, |\mathbf{U}|) + \xi_a \ , \tag{9}$$

$$\gamma_o \frac{dT_o}{dt} = -f(T_a, T_o, |\mathbf{U}|) - \lambda_o(T_o - T_{o_e}) + \xi_o \equiv F_o(T_a, T_o, |\mathbf{U}|) + \xi_o \ , \tag{10}$$

where $f(T_a, T_o, |\mathbf{U}|)$ is the latent and sensible heat flux through the air-sea interface which depends on T_o, T_a, and wind speed $|\mathbf{U}|$. External forcings of T_a and T_o (that is, forcing not due explicitly to air-sea interaction) are represented by ξ_a and ξ_o, respectively. The remaining terms $-\lambda_a(T_a - T_{a_e})$ and $-\lambda_o(T_o - T_{o_e})$ represent the effective (basically long wave) damping of each component to equilibrium temperatures T_{a_e} and T_{o_e}. From hereon, the equilibrium temperature terms will be included in ξ_a and ξ_o. The bulk formula for the heat flux f is

$$f = \beta(T_o - T_a)|\mathbf{U}| \ , \tag{11}$$

where β is a parameter that depends upon the bulk transfer coefficients and the inverse Bowen ratio (ratio of latent to sensible heat flux). That is, we assume that the heat flux variability is only due to AIRT, SST, and wind speed variability. This is a reasonable approximation in our simple framework, since cold season heat flux anomalies are strongly related to wind speed anomalies (e.g., Ronca and Battisti 1997; Alexander and Scott 1997). It is not a perfect approximation, of course. In particular, we make the key simplifying assumption that the sensible and latent heat fluxes can be combined together into one term in the bulk heat flux formula (11) (as, e.g., Frankignoul and Hasselmann 1977), removing humidity as an explicit variable. Note that, for the uncoupled problem, SNA found that this simplification affected the results quantitatively but did not obscure the main points drawn from the derivation using (11); that is, the fundamental nature of multiplicative noise can be established from (11) since it contains the basic physics involved in local air-sea coupling.

3.2 Taylor expansion

A Taylor expansion of the right hand sides of (9) and (10) with respect to $T_a = \overline{T}_a + T'_a$ and $T_o = \overline{T}_o + T'_o$ yields

$$\gamma_a \frac{d(\overline{T_a} + T'_a)}{dt} = F_a(\overline{T_a}, \overline{T_o}, |\mathbf{U}|) + \frac{\partial F_a}{\partial T_a} T'_a + \frac{\partial F_a}{\partial T_o} T'_o + \overline{\xi_a} + \xi'_a + O(T'^2_a, T'^2_o) \ , \tag{12}$$

$$\gamma_o \frac{d(\overline{T_o} + T'_o)}{dt} = F_o(\overline{T_a}, \overline{T_o}, |\mathbf{U}|) + \frac{\partial F_o}{\partial T_a} T'_a + \frac{\partial F_o}{\partial T_o} T'_o + \overline{\xi_o} + \xi'_o + O(T'^2_a, T'^2_o) \ , \tag{13}$$

where (T_a-dimension)

$$F_a(\overline{T_a}, \overline{T_o}, |\mathbf{U}|) \ = \ \beta(\overline{T_o} - \overline{T_a})|\mathbf{U}| - \lambda_a \overline{T_a} \ ,$$

$$\begin{aligned} \frac{\partial F_a}{\partial T_a} T'_a &= (-\beta|\mathbf{U}| - \lambda_a) T'_a \ , \\ \frac{\partial F_a}{\partial T_o} T'_o &= \beta|\mathbf{U}| T'_o \ , \end{aligned} \tag{14}$$

and (T_o-dimension)

$$\begin{aligned} F_o(\overline{T_a}, \overline{T_o}, |\mathbf{U}|) &= -\beta(\overline{T_o} - \overline{T_a})|\mathbf{U}| - \lambda_a \overline{T_o} \ , \\ \frac{\partial F_o}{\partial T_a} T'_a &= \beta|\mathbf{U}| T'_a \ , \\ \frac{\partial F_o}{\partial T_o} T'_o &= (-\beta|\mathbf{U}| - \lambda_o) T'_o \ , \end{aligned} \tag{15}$$

overbars represent means and primes represent anomalies, and $O(T_a'^2, T_o'^2)$ represents all higher order terms in the Taylor's expansion. The derivation is further simplified by setting β to a constant. In reality, β depends somewhat on the air-sea temperature difference $T_o - T_a$ (the stability) and the strength of the wind speed $|\mathbf{U}|$ (e.g., Large and Pond 1982), but again SNA found that ignoring the dependence upon stability has some quantitative but little qualitative impact on the results. For constant β, F_a and F_o have only quadratic nonlinearities, so that there are no higher order terms in (12) and (13) and thus there is no restriction on the magnitudes of the temperature anomalies.

The time mean of (12) and (13) produces

$$\gamma_a \frac{d\overline{T_a}}{dt} = \beta(\overline{T_o} - \overline{T_a})|\mathbf{U}| - \lambda_a \overline{T_a} + \beta\overline{|\mathbf{U}|'(T'_o - T'_a)} + \overline{\xi_a} \ , \tag{16}$$

$$\gamma_o \frac{d\overline{T_o}}{dt} = -\beta(\overline{T_o} - \overline{T_a})|\mathbf{U}| - \lambda_a \overline{T_a} - \beta\overline{|\mathbf{U}|'(T'_o - T'_a)} + \overline{\xi_o} \ , \tag{17}$$

Subtracting (16) and (17) from (12) and (13) results in the coupled set of equations for the anomalous temperatures T'_a and T'_o:

$$\gamma_a \frac{dT'_a}{dt} = \qquad \beta(\overline{T_o} - \overline{T_a})|\mathbf{U}|' - \left[\beta(\overline{|\mathbf{U}|} + |\mathbf{U}|') + \lambda_a\right] T'_a + \beta(\overline{|\mathbf{U}|} + |\mathbf{U}|') T'_o$$

$$- \quad \beta\overline{|\mathbf{U}|'(T_o' - T_a')} + \xi_a' \quad , \tag{18}$$

$$\gamma_o \frac{dT_o'}{dt} = \quad - \quad \beta(\overline{T_o} - \overline{T_a})|\mathbf{U}|' + \beta(\overline{|\mathbf{U}|} + |\mathbf{U}|')T_a' - \left[\beta(\overline{|\mathbf{U}|} + |\mathbf{U}|') + \lambda_o\right] T_o'$$
$$+ \quad \beta\overline{|\mathbf{U}|'(T_o' - T_a')} + \xi_o' \quad . \tag{19}$$

Apart from anomalous external forcing, which for simplicity hereon is assumed to be additive noise, perturbations in this simple model are only due to heat flux anomalies induced by either the mean wind or the anomalous wind. Typically, the ratio of daily averages of mean and anomalous wind speeds is only about 2 to 1 (e.g., Monahan 2006b). As a consequence, a scale analysis of the flux terms (SNA) shows that the terms depending upon the wind speed anomalies $|\mathbf{U}|'$ are too large to ignore.

We now assume that $|\mathbf{U}|'$ can be approximated by Gaussian white-noise. This assumption is justifiable if $|\mathbf{U}|'$ varies much more rapidly than SST and AIRT and if it has a distribution that is nearly Gaussian. For example, at OWS P daily wind speed anomalies have a 1-day autocorrelation time-scale (Fig. 2a) and deviations from Gaussianity are relatively small (Fig. 2b). However, while SST has an autocorrelation time-scale of a few months, AIRT has only about a 3.5-day autocorrelation time-scale, so that while the white-noise approximation of wind speed is excellent compared to SST it may be only fair compared to AIRT. This issue can be partly addressed by simply scaling the white-noise amplitude by the square root of the wind speed time-scale (Sardeshmukh et al. 2001). Perhaps a better approximation of wind speed would be to represent it as red-noise with a short decorrelation time, but this correction may be relatively minor for the values considered herein given a previous analysis of multiplicative red-noise in a system similar to that discussed below (Sardeshmukh et al.

2003).

Employing the Gaussian white-noise assumption for wind speed and absorbing the mean forcing in the definition of the anomalies, (18) and (19) become stochastic differential equations (SDEs) that in matrix form are expressed as

$$\frac{d\mathbf{T}'}{dt} = \mathbf{A}\mathbf{T}' + \mathbf{B}_M(\mathbf{T}')\boldsymbol{\eta}_M + \mathbf{B}_A\boldsymbol{\eta}_A \ , \tag{20}$$

with the 2×2 matrices

$$\mathbf{A} = \begin{pmatrix} -(\frac{\beta}{\gamma_a}\overline{|\mathbf{U}|} + \frac{\lambda_a}{\gamma_a}) & \frac{\beta}{\gamma_a}\overline{|\mathbf{U}|} \\ \frac{\beta}{\gamma_o}\overline{|\mathbf{U}|} & -(\frac{\beta}{\gamma_o}\overline{|\mathbf{U}|} + \frac{\lambda_o}{\gamma_o}) \end{pmatrix} \equiv \begin{pmatrix} -a & b \\ c & -d \end{pmatrix} \tag{21}$$

and

$$\mathbf{B}_M(\mathbf{T}') = \begin{pmatrix} \frac{\sigma^M\beta}{\gamma_a}(T_o' - T_a' + \Pi) & 0 \\ \frac{\sigma^M\beta}{\gamma_o}(T_a' - T_o' - \Pi) & 0 \end{pmatrix} \equiv \begin{pmatrix} B_{11}(T_a', T_o') & 0 \\ B_{21}(T_a', T_o') & 0 \end{pmatrix} \ . \tag{22}$$

The state vector is $\mathbf{T}' = (T_a', T_o')^T$, and the mean SST-AIRT temperature difference is $\Pi = \overline{T_o} - \overline{T_a}$. Note that the absorption of the mean forcing in the definition of the anomalies is a simple stochastic renormalization procedure, which does not impact the dynamics of SST and AIRT variability. There are two sources of noise: the additive stochastic noise vector $\boldsymbol{\eta}_A = (\eta_{T_a}^A, \eta_{T_o}^A)^T$ multiplied by an amplitude matrix $\mathbf{B}_A$ that can have non-zero off-diagonal elements, and multiplicative noise resulting from the matrix $\mathbf{B}_M(\mathbf{T}')$ multiplied by the noise vector $\boldsymbol{\eta}_M = (\eta_{T_a}^M, 0)^T$. The variance of $|\mathbf{U}|'$ is absorbed in the constant σ^M, in the manner discussed by Sardeshmukh et al. (2001), so that $\eta_{T_a}^M$ has unit variance. The stochastic components are assumed to be independent, normalized Gaussian white-noise processes.

Without multiplicative noise ($\mathbf{B}_M \equiv 0$), (20) is structurally equivalent to the system used by BB98, except they assumed no white-noise forcing of SST. With multiplicative noise, the

system can result in non-Gaussian PDFs of $\mathbf{T}'$. However, if $\Pi \equiv 0$, the multiplicative noise is symmetric about $T_a' = T_o' = 0$ and will only produce symmetric (not skewed) non-Gaussian distributions. That is, the $\Pi\,\eta_{T_a}^M$ terms in $\mathbf{B}_M(\mathbf{T}')$, which represent additive noise that is correlated with the multiplicative noise, induce skewness. This is consistent with the mixed-layer single column model results in SNA, where the skewness of SST anomalies was largely due to the mean AIRT-SST difference. On the other hand and unlike our bivariate model, their simple univariate theoretical model did not include T_a explicitly, so it did not contain correlated additive and multiplicative noise components and consequently could not produce skewness.

Because a rapidly fluctuating quantity ($|\mathbf{U}|'$) with a small but finite correlation time is approximated as white-noise, (20) has to be treated as a Stratonovich SDE. As we have already heuristically explained in section 2, the multiplicative noise in a Stratonovich system induces a *noise-induced drift*. Here the corresponding noise-induced drift [see (A.3)] is

$$\frac{1}{2}\left(\frac{\partial B_{11}}{\partial T_a'}\right) B_{11} + \frac{1}{2}\left(\frac{\partial B_{11}}{\partial T_o'}\right) B_{21} = -\frac{1}{2}\frac{(\sigma^M\beta)^2}{\gamma_a^2}(T_o' - T_a' + \Pi) - \frac{1}{2}\frac{(\sigma^M\beta)^2}{\gamma_a\gamma_o}(T_o' - T_a' + \Pi) \quad (23)$$

for the T_a'-component, and

$$\frac{1}{2}\left(\frac{\partial B_{21}}{\partial T_a'}\right) B_{11} + \frac{1}{2}\left(\frac{\partial B_{21}}{\partial T_o'}\right) B_{21} = \frac{1}{2}\frac{(\sigma^M\beta)^2}{\gamma_a\gamma_o}(T_o' - T_a' + \Pi) + \frac{1}{2}\frac{(\sigma^M\beta)^2}{\gamma_o^2}(T_o' - T_a' + \Pi) \quad (24)$$

for the T_o'-component. Noting that the atmospheric heat capacity is much smaller than oceanic heat capacity (that is, $\gamma_a \ll \gamma_o$) the second terms on the right hand sides can be neglected:

$$\frac{1}{2}\left(\frac{\partial B_{11}}{\partial T_a'}\right) B_{11} + \frac{1}{2}\left(\frac{\partial B_{11}}{\partial T_o'}\right) B_{21} \approx -\frac{1}{2}\frac{(\sigma^M\beta)^2}{\gamma_a^2}(T_o' - T_a' + \Pi) \quad (25)$$

for the T'_a-component, and

$$\frac{1}{2}\left(\frac{\partial B_{21}}{\partial T'_a}\right)B_{11}+\frac{1}{2}\left(\frac{\partial B_{21}}{\partial T'_o}\right)B_{21}\approx\frac{1}{2}\frac{(\sigma^M\beta)^2}{\gamma_a\gamma_o}(T'_o-T'_a+\Pi) \tag{26}$$

for the T'_o-component.

Figure 3 summarizes the distinction made above between *air-sea interaction with mean wind only* (upper panel) and *air-sea interaction with mean and fluctuating winds* (lower panel). The physical set-ups are shown on the left hand sides of each panel, while the equivalent mathematical relations are depicted on the panel's right hand sides. In both cases (upper and lower panels) the oceanic and atmospheric temperatures are radiatively damped. When only the mean wind drives heat flux (upper panel), the heat flux coupling is $\pm\beta(T_o-T_a)\overline{|\mathbf{U}|}$ and the evolution of SST and AIRT is given by the deterministic drift matrix $\mathbf{A}$ with parameters $-a, b, c, -d$. This is depicted by the corresponding arrows: $-a$ damps the atmosphere, b is the oceanic forcing of the atmosphere, c is the atmospheric forcing of the ocean, and $-d$ damps the ocean. When the heat flux is instead due to both the mean and fluctuating winds, the predictable evolution of atmosphere-ocean temperatures is given by the *effective* drift matrix

$$\tilde{\mathbf{A}}=\begin{pmatrix} -a+\frac{1}{2}\frac{(\sigma^M\beta)^2}{\gamma_a^2} & b-\frac{1}{2}\frac{(\sigma^M\beta)^2}{\gamma_a^2} \\ c-\frac{1}{2}\frac{(\sigma^M\beta)^2}{\gamma_a\gamma_o} & -d+\frac{1}{2}\frac{(\sigma^M\beta)^2}{\gamma_a\gamma_o}\end{pmatrix}\equiv\begin{pmatrix} -\tilde{a} & \tilde{b} \\ \tilde{c} & -\tilde{d}\end{pmatrix}\ . \tag{27}$$

That is, the multiplicative noise results in a noise-induced drift [see Eqs. (25) and (26)] that effectively decreases the amplitudes of the damping and coupling parameters, altering the predictable dynamics of air-sea interaction. In particular, multiplicative noise leads to effectively reduced damping through its effect on $\tilde{a}$ and $\tilde{d}$, yet simultaneously effectively

weakens air-sea coupling and thus weakens the (coupling-induced) reduced thermal damping proposed by BB98. Very strong multiplicative noise could even, in principle, cause a change in sign of the coefficients of $\tilde{\mathbf{A}}$, as long as the system is not destabilized for long periods of time. In effect, rapid fluctuations in wind speed act to somewhat insulate the atmosphere and ocean from each other.

4 Parameter estimation from observations

To gauge the effect of multiplicative noise on atmosphere-ocean coupling, we next estimate the parameters of the simple coupled model (20) from Ocean Weather Station (OWS) data. Of all the Ocean Weather Stations, OWS P may be best suited for this purpose (Hall and Manabe 1997; Sura et al. 2006). It has a long high-quality record, the El Niño-Southern Oscillation (ENSO) signal is relatively weak there (e.g., Alexander et al. 2002), and it is located far from strong currents. We will, therefore, in the following provide a detailed discussion of OWS P (see Table 1) as our "prototype" for midlatitude, wintertime atmosphere-ocean coupling. A brief discussion of results from shorter-record stations is presented at the end of this section.

4.1 Data

Daily SST and AIRT anomalies were determined as follows. First, daily averages were calculated from the raw 3-hourly data. Then the climatological monthly averages were estimated. A daily climatology was constructed by linear interpolation using these monthly

averages as base points. Finally, daily anomalies were calculated by subtracting the daily climatology from the mean daily values.

SNA have already shown that SST variability is best described by a stochastic model of surface heat fluxes during the extended wintertime (November-April), since the anomalous mixed-layer temperature (SST) tendency is predominantly due to the net turbulent heat flux anomalies and not to changes in the mixed-layer depth (Alexander and Penland 1996; Sura et al. 2006). Also, radiative flux anomalies have only a minor impact during the cold season (Park et al. 2005; Frankignoul and Kestenare 2002). Therefore, the following analysis is restricted to the extended winter season.

4.2 Parameter estimation

The most general expression of a bivariate SDE that governs the evolution of AIRT and SST anomalies is

$$\frac{d\mathbf{T}'}{dt} = \mathbf{A}(\mathbf{T}') + \mathbf{B}(\mathbf{T}')\boldsymbol{\eta} \tag{28}$$

(see appendix), where we have not yet made assumptions about the forms of the deterministic operator $\mathbf{A}$ and stochastic operator $\mathbf{B}$. To determine parameters for the model (20), then, we also need to show that $\mathbf{A}$ and $\mathbf{B}$ take the forms given by (20-22). The direct finite-difference technique [(A.5); see appendix] is used to estimate $\mathbf{A}(\mathbf{T}')$ at OWS P; results are shown in Figs. 4a and 4b. In principle, this technique can determine either linear or non-linear drifts. However, Fig. 4 shows the drift is nearly linear, suggesting that the linear approximation of (20) and (27) [and earlier used by Barsugli and Battisti (1998)] is a good approximation of

the real system; that is, $\mathbf{A}(\mathbf{T}') \approx \mathbf{A}\mathbf{T}'$. Thus, we recalculated the linear effective drift matrix for OWS P, which is:

$$\tilde{\mathbf{A}} = \begin{pmatrix} -0.35 & 0.22 \\ 0.01 & -0.04 \end{pmatrix} \quad . \tag{29}$$

The method used to estimate the multiplicative noise matrix $\mathbf{B}\mathbf{B}^T$ is similar to that used to estimate the drift. However, as noted in the appendix, estimation of the former is more prone to error. The most practical way to detect the systematic error made by using a finite time step is to examine the results to changing Δt (Sura and Barsugli 2002). Unfortunately, because the components of $\mathbf{B}\mathbf{B}^T$ vary over more than two orders of magnitude, only the largest component $(\mathbf{B}\mathbf{B}^T)_{11}$, shown in Fig. 4c, can be determined with confidence. Even then, there is some uncertainty in an overall constant; that is, the gradient of $(\mathbf{B}\mathbf{B}^T)_{11}$ (which represents the multiplicative noise) is much less sensitive to varying Δt than is the vertical offset (which represents the additive noise), a result consistent with the findings in Sura and Barsugli (2002). This uncertainty in the non-parametric estimation of the vertical offset [(A.6)] can be overcome by instead determining the additive noise from the fluctuation-dissipation relation, which requires the noise to reproduce the observed covariance structure (see (35) below). As a caveat, note that all the stochastic parameters determined using the above method are meant to be rough estimates, having uncertainties up to a factor of two. However, the results shown below are reasonably robust to factor of two variations in the parameters, suggesting that this analysis captures the basic underlying stochastic physics.

Recall that in the simple model of section 3, $(\mathbf{B}\mathbf{B}^T)_{11} = (B_{11})^2$ [cf. (22)]. Fig. 4c shows that the observed $(\mathbf{B}\mathbf{B}^T)_{11}$ has a structure quite similar to $(B_{11})^2$ predicted by the model,

with a pronounced minimum for $T'_o - T'_a \approx -0.7\mathrm{K} = \Pi$ and a roughly quadratic increase orthogonally away from the minimum line. It is thus reasonable to use $(\mathbf{B}\mathbf{B}^T)_{11}$ to estimate the parameters of the linear multiplicative noise terms in (20). First, given (22), $\left(\sigma^M\beta/\gamma_a\right)^2$ can be estimated from the gradient in Fig. 4c. Next, the ratio γ_a/γ_o is given by the ratio $\tilde{c}/\tilde{b}$ [see (27)]. Given $\left(\sigma^M\beta/\gamma_a\right)^2$ the ratio γ_a/γ_o is then used to calculate $\left(\sigma^M\beta/\sqrt{\gamma_a\gamma_o}\right)^2$ and $\left(\sigma^M\beta/\gamma_o\right)^2$. This procedure results in the following estimates:

$$\gamma_a/\gamma_o \approx 0.05 \ , \tag{30}$$

$$\left(\sigma^M\beta/\gamma_a\right)^2 \approx 0.2 \ , \tag{31}$$

$$\left(\sigma^M\beta/\sqrt{\gamma_a\gamma_o}\right)^2 \approx 0.01 \ , \tag{32}$$

$$\left(\sigma^M\beta/\gamma_o\right)^2 \approx 0.0005 \ . \tag{33}$$

γ_a/γ_o determined in this manner is identical to that used by BB98, where it was determined as the ratio of the heat capacities of a dry tropospheric column and oceanic mixed-layer with depth of about 50 m. The actual mixed-layer depth at OWS P during winter is larger by about a factor of 2, but given the limitations of our simple model (for example, the effective heat capacity of the atmospheric column could be greater due to effects of moisture content and atmospheric heat transport processes ignored here) γ_a/γ_o seems of reasonable value. The other parameters are consistent with typical values of β and wind speed variability at OWS P. From (22), the covariance of the multiplicative noise is then

$$\langle \mathbf{B}_M \mathbf{B}_M^T \rangle = \begin{pmatrix} 0.48 & -0.024 \\ -0.024 & 0.0012 \end{pmatrix} \ . \tag{34}$$

Given the multiplicative noise, the additive noise required to reproduce the observed covariance structure can now be calculated from the fluctuation-dissipation relation (see

appendix),

$$\mathbf{B}_A\mathbf{B}_A^T = -\tilde{\mathbf{A}}\mathbf{C}_0 - \mathbf{C}_0\tilde{\mathbf{A}} - \langle \mathbf{B}_M\mathbf{B}_M^T \rangle \ , \tag{35}$$

where $\mathbf{C}_0$ is the data's covariance matrix at lag zero, yielding

$$\mathbf{B}_A\mathbf{B}_A^T = \begin{pmatrix} 0.92 & 0.07 \\ 0.07 & 0.03 \end{pmatrix} \ . \tag{36}$$

Note that the multiplicative noise comprises about one third of the overall atmospheric noise forcing but is an almost negligible component of SST noise forcing. Also, while the pure additive noises of SST and AIRT have a 0.4 correlation, SST and AIRT multiplicative noises are anticorrelated, so that overall SST and AIRT noises have only a 0.2 correlation.

Finally, the deterministic drift is calculated as the difference between the effective drift (29) and the noise-induced drift [using (30-33) in (27)]:

$$\mathbf{A} = \begin{pmatrix} -0.45 & 0.32 \\ 0.015 & -0.045 \end{pmatrix} \ . \tag{37}$$

Comparison of $\mathbf{A}$ and $\tilde{\mathbf{A}}$ suggests that the noise-induced drift reduces the effective coupling by roughly one third, and decreases the effective damping by roughly 10% for SST and 20% for AIRT.

4.3 Testing the multiplicative white-noise model

We next test if the two assumptions of linear dynamics and the white-noise approximation made in (20) are consistent with the data from OWS P. For any observation $\mathbf{T'}_{obs}(t)$ the effective drift $\tilde{\mathbf{A}}\mathbf{T'}_{obs}(t)$ estimated from data can be used to calculate a forward time step

Δt: $\mathbf{T}'(t+\Delta t) = \tilde{\mathbf{A}}\mathbf{T}'_{obs}(t)\Delta t + \mathbf{T}'_{obs}(t)$. If the white-noise assumption is correct the residual

$$\mathbf{r} \equiv \mathbf{T}'_{obs}(t+\Delta t) - \mathbf{T}'(t+\Delta t) \tag{38}$$

should equal the white-noise terms in (20). Autocorrelation functions and PDFs of the residual are shown in Fig. 5. For both AIRT and SST anomalies the autocorrelations are close to zero after one time step of 1 day. That is, the residuals are practically uncorrelated on the resolved time scale, consistent with the white-noise approximation. Moreover, the PDFs of the residuals are non-Gaussian, indicating that multiplicative white-noise is essential to represent the noise in the coupled system. In particular, the PDF of the SST residual is very close to an exponential distribution (straight line in logarithmic plot) and thus highly non-Gaussian (discussed in more detail in SNA). On the other hand, the PDF of the AIRT residual is closer to a Gaussian, but still shows a heavy non-Gaussian tail for negative residuals.

Not only are the residuals uncorrelated after a day, but there is also no significant long range correlation in Fig. 5a, confirming that the linear model of local air-sea interaction is a good approximation of the observed coupled thermodynamics at OWS P. Note, however, that the assumption of additive Gaussian white-noise made in the BB98 model (and also, e.g., Mosedale et al. 2005) appears invalid.

4.4 Probability Density Functions

As a hard test of our simple coupled multiplicative noise model, we next examine if it reproduces the observed joint PDF of AIRT and SST anomalies at OWS P. Deviations from

Gaussianity of PDFs can shed light on the underlying dynamics of stochastic systems (e.g., Peinke et al. 2004; Sura et al. 2005). A parametric method is used to calculate the joint PDFs of observed (and modeled) AIRT and SST anomalies, in which the parameters of a "skew-t" distribution are determined by a Maximum Likelihood Estimate (MLE). The skew-t distribution, a skewed and kurtosed alternative to the normal distribution, is used because it is capable of adapting very closely to skewed and heavy-tailed data (Azzalini and Capitanio 2003; Jones and Faddy 2003; Azzalini 2005; R Development Core Team 2004). By comparing a simple histogram to the skew-t estimate, SNA showed that the skew-t distribution excellently represents the marginal PDF of observed SST anomalies. Similarly, for the joint PDFs the skew-t distribution captures the structure of the 2-d histograms very well (not shown).

The joint PDF anomalies (deviations from Gaussianity) of our simple model are shown in Fig. 6a, whereas the observed joint PDF anomalies are shown in Fig. 6b. Here we normalized the anomaly timeseries to have zero means and unit variances to make the comparison of the PDFs easier to view.

The basic non-Gaussian structures and their amplitudes are the same in both the model and the observations. The joint PDF is stronger than Gaussian around the origin, has weak flanks on both sides of the peak (weaker for negative AIRT anomalies than for positive ones), and has heavy tails (not well seen here because of the contour levels used). The maxima of both the modeled and observed PDF anomalies lie shifted into the positive AIRT-plane, consistent with the effect of the mean air-sea temperature difference in the multiplicative noise. These results are reasonably robust, to factor of two variations in

the parameters (30-33). The main difference between the model and observations is in the positive AIRT half-plane, where there is a slight mismatch of the PDF anomaly's orientation and amplitude. This mismatch may be due to the simplicity of the model; for example, the stability dependence of the bulk flux parameter β was neglected, but in reality the value should be different for $T_a > T_o$ and $T_a < T_o$ (e.g., Large and Pond 1982, see also the discussion of the model results in SNA). Still, given the simplicity of the model the agreement of the simulated and observed joint PDFs in Fig. 6 is remarkably good. The main point is that the effective deterministic drift of our model is linear and that parameterizing state-dependent rapidly-varying heat flux with multiplicative noise can explain the observed non-Gaussian statistics.

4.5 Spectra

The impact of multiplicative noise upon the variability of AIRT and SST anomalies is demonstrated by numerically integrating two different coupled stochastic models, with and without multiplicative noise. To do so, we integrate (20) forwards for 10^6 days (the "multiplicative noise model"), and then repeat the calculations by removing all multiplicative noise terms (the "additive noise model"). The crucial difference is that while both model runs have the same deterministic dynamics, the additive noise model does not have the noise-induced drift. In addition, the overall variance of modeled anomalous AIRT and SST variability is reduced in the additive noise model because the strength of the noise forcing itself is reduced. More precisely, the observed covariance structure of AIRT and SST variability is not conserved in the additive noise model. This experiment visualizes the bias one might get, for example, in

the extreme case of a coupled model failing to reproduce rapidly decorrelating (in time) sea surface winds.

The spectra for this set of model runs are shown in Fig. 7, for AIRT (top) and SST (bottom). The spectra of the additive noise model are indicated by the dashed lines, and the spectra of the full multiplicative noise model are indicated by the solid lines. Consistent with the amplitude of the noise-induced drift found in section 4.2, the removal of the multiplicative noise has a much larger impact on the AIRT spectrum than the SST spectrum. AIRT variance decreases by about 35%, with most of this impact evident on the subseasonal timescale, where variance decreases by about 45% and the peak in the spectrum shifts to shorter periods. Conversely, the effect of multiplicative noise is much less on periods of months to years. That is, the multiplicative noise has an impact not just on the overall variance but on the shape of the power spectrum, leading to relatively more subseasonal variability.

Multiplicative noise has two effects upon SST, leading to the change between the two curves in Fig. 7b. First, the noise-induced drift weakens the effective damping of SST and thus acts to increase SST variance. If only this effect is removed, SST variance is reduced by about 10% (not shown) in the additive noise model, consistent with the results in SNA. However, removing multiplicative noise also reduces AIRT variance, so consequently the forcing of SST by the atmosphere is reduced. Note that the red-noise structure of the SST spectrum is not visibly altered by the multiplicative noise.

4.6 Other Ocean Weather Stations

We repeated the analysis performed upon OWS P for two other stations with shorter data records: OWS N in the North Pacific and OWS K in the North Atlantic (see Table 1 for the exact locations). These stations are both in midlatitudes and far away from strong currents. Therefore, we expect to see rather similar characteristics at OWS P, N, and K.

The observed joint PDFs at OWS K and N are shown on the left hand sides of Figs. 8a and b. The joint PDF at OWS K (Fig. 8a, left hand side) is indeed similar to the PDF observed at OWS P (Fig. 6b), albeit with the SSTs slightly more kurtosed and skewed. The joint PDF at OWS N (Fig. 8b, left hand side) also shows a similar structure, but the deviation from Gaussianity is notably rotated so that the non-Gaussianity is much stronger in the direction of the SST-axis (consistent with the marginal SST PDFs shown in SNA).

The modeled joint PDFs at OWS K and N are shown on the right hand sides of Figs. 8a and b. The simple stochastic model reproduces the joint PDF at OWS K relatively well (Fig. 8a), including the slight rotation of the PDF relative to OWS P. In fact, all the parameters at OWS K are broadly similar to the parameters determined at OWS P. At OWS N the model reproduces the basic structure, but captures only some of the rotation of the observed PDF (Fig. 8b). In the model, such clockwise rotation of the PDF anomaly occurs because of an increase in the estimated γ_a/γ_o (≈ 0.2 at OWS N), which results in relatively more multiplicative noise forcing of SST [e.g., in (19)]. Although the failure of the model to completely reproduce the OWS N PDF might be due to the difficulty of estimating parameters from the shorter data record, it seems more likely a result of a deficiency of the

model itself. Notably, the model combines latent and sensible heat fluxes together using the Bowen ratio formulation and then parameterizes the heat flux solely as a function of the air-sea temperature difference. Strictly speaking, however, the latent heat flux is a function of the dewpoint as well. Since OWS N is further south than OWS P and K, the latent heat flux there is relatively more important (e.g., Alexander and Scott 1997), and may need to be treated separately rather than combined with sensible heat flux as in our model. Also, recall that the skew in this model is due to the mean stability parameter Π, which determines the amount of additive noise correlated with the multiplicative noise in $\mathbf{B}_M(\mathbf{T}')$. For the latent heat flux, the relevant parameter is instead the difference between the mean SST and mean dewpoint temperature. This difference is twice as large at OWS N as at OWS P, so the fraction of correlated additive noise might be underestimated by a model that focuses on the mean AIRT-SST difference alone. Other physical processes not considered in our simple model that result in more correlated additive noise might also be particularly important at this location.

The key point, however, is that the multiplicative noise physics and the related non-Gaussianity at OWS P are not unique but also appear relevant at other midlatitude stations. This adds confidence to the ability of the model to capture the basic mechanism through which rapid wind variability impacts air-sea thermal coupling.

5 Summary and conclusions

In this paper we investigated how air-sea thermal coupling is impacted by the presence of rapidly varying surface winds, an effect generally ignored in past studies. By representing the rapidly-varying winds as white-noise within a bulk formulation of surface turbulent heat fluxes, an equation for the coupled AIRT-SST system is derived that notably includes a stochastic process depending upon the atmospheric and oceanic thermal anomalies themselves. This state-dependent, or multiplicative, noise alters the predictable dynamics of atmosphere-ocean coupling because it induces an additional heat flux term, the noise-induced drift, that acts to effectively weaken coupling but also to effectively weaken dissipation. For example, at OWS P the noise-induced drift results in about a one-third decrease of the effective coupling parameters, and about a 10-20% decrease of the effective damping parameters. In general, the effect of reduced thermal damping is weakened by noise in the coupling coefficients, one possible reason why the empirically determined effective coupling parameters for all three Ocean Weather Stations are much weaker than those used by BB98. Thus, while multiplicative noise acts to *increase* the persistence of SST and AIRT anomalies by reducing the damping of each, it simultaneously acts to *decrease* the persistence by weakening the air-sea coupling.

Our analysis has focused on how rapid wind variability alone results in multiplicative noise in the surface heat flux. Our model is quite simple, and in particular does not include any possible dynamical response of the atmosphere to SST anomalies (e.g., Neelin and Weng 1999), especially in the surface wind variability itself. Surface thermal and wind anomalies might also be correlated if anomalies in low-level stability (e.g., in the air-sea temperature

difference) significantly affects surface winds through changes in the downward turbulent mixing of momentum (Chelton et al. 2004; O'Neill et al. 2003; Small et al. 2005; Xie 2004). As SNA had previously found, explicit consideration of the latent heat flux dependence upon dewpoint, and bulk coefficients dependence upon stability, might also refine the model. Other physical processes not considered here may also be at least partly represented by multiplicative and/or correlated additive noise components related to both wind and thermal anomalies. For example, radiative forcing due to clouds (especially in the marine stratocumulus regions beneath the subtropical highs) and variations in the mixed layer depth may both have a surface wind dependence, although these processes may be primarily relevant during the warm season. Given these limitations, it is a striking result that the inclusion of this simple multiplicative noise term allows our model to reproduce not only the autocorrelation functions of SST and AIRT anomalies, but also the main non-Gaussian features of the observed joint PDFs. Moreover, our model predicts that the multiplicative noise will be linearly dependent upon the surface air-sea temperature difference, a result that is confirmed by observations. This agreement with observations suggests that our model captures the basic impact of rapid wind variability upon air-sea thermal coupling.

An important consequence of the theory outlined here is that air-sea coupling includes both deterministic and stochastic components. That is, rapidly varying boundary-layer winds and related heat fluxes are unpredictable on the longer dynamical time-scales of the ocean yet are a crucial component of atmosphere-ocean coupling, and may not be just averaged away. Note that by modeling winds as "rapid" white-noise, our analysis can not determine the relative importance of synoptic variability of the wind field versus mesoscale

variability and wind gustiness. Still, there is clearly a significant scale interaction between the fast wind induced heat flux variability and the slower AIRT and SST variability. This interaction must be captured by coupled models if they are to produce realistic atmosphere-ocean coupling and correct estimates of AIRT and SST climate variability, and even mean climate states. For example, the many atmospheric models that significantly underestimate wind variability in the marine boundary layer (e.g., Gille 2005; Monahan 2006a,b) might be expected to also underestimate rapid flux variability and, as a result of the noise-induced drift, potentially overestimate the strength of air-sea coupling. More generally, how a bias in wind variability (and related heat fluxes) contributes to biases found in many coupled models is likely to be a complex issue. However, we have a powerful theory/tool at hand to systematically study this problem. The results could guide the development of improved coupling schemes and the implementation of stochastic parameterizations in climate models.

Acknowledgments. The authors thank Dr. Adam Monahan and one anonymous reviewer whose comments greatly improved the paper. This work was supported by a grant from NOAA CLIVAR/Pacific and NSF grant 0552047.

Appendix

Stochastic dynamics in a nutshell

This appendix reviews a few basic ideas of stochastic dynamics used in this paper. More comprehensive treatments may be found in many textbooks (e.g., Gardiner 2004; Horsthemke and Léfèver 1984; Paul and Baschnagel 1999).

Consider the dynamics of an n-dimensional system whose state vector $\mathbf{x}$ is governed by the stochastic differential equation (SDE)

$$\frac{d\mathbf{x}}{dt} = \mathbf{A}(\mathbf{x}) + \mathbf{B}(\mathbf{x})\boldsymbol{\eta} \tag{A.1}$$

where the vector $\mathbf{A}$ represents all slow (deterministic) processes and $\mathbf{B}(\mathbf{x})\boldsymbol{\eta}$, with the matrix $\mathbf{B}$ and the noise vector $\boldsymbol{\eta}$, represents the stochastic approximation to the fast nonlinear processes. The stochastic components η_i are assumed to be independent Gaussian white noise processes:

$$\langle \eta_i(t) \rangle = 0, \qquad \langle \eta_i(t)\eta_i(t') \rangle = \delta(t - t') \tag{A.2}$$

where $\langle ... \rangle$ denotes the averaging operator. The corresponding Fokker-Planck equation,

$$\begin{aligned} \frac{\partial p(\mathbf{x},t)}{\partial t} = & - \sum_i \frac{\partial}{\partial x_i} \left[A_i + \alpha \sum_{j,k} \left(\frac{\partial}{\partial x_j} B_{ik} \right) B_{jk} \right] p(\mathbf{x},t) \\ & + \frac{1}{2} \sum_{i,j} \frac{\partial^2}{\partial x_i \partial x_j} (\mathbf{B}\mathbf{B}^T)_{ij} p(\mathbf{x},t) \, , \end{aligned} \tag{A.3}$$

describes the conservation of the probability density $p(\mathbf{x}, t)$ of the system described by the SDE (A.1). Two different values of α yield two physically important stochastic calculi: the Itô ($\alpha = 0$) and the Stratonovich calculus ($\alpha = 1/2$). On the right hand side, the first term

within square brackets describes the dynamics of the deterministic system and is called the deterministic drift. The second term within square brackets, which does not occur in Itô systems ($\alpha = 0$), is called the noise-induced drift. The remaining term is associated with the diffusion of the probability density by noise.

For a detailed discussion of stochastic integration and the differences between Itô and Stratonovich SDEs see for example Horsthemke and Léfèver (1984), Gardiner (2004), or Penland (1996). The key point here is that the Stratonovich calculus is relevant for continuous physical systems, such as the atmosphere, in which rapidly fluctuating quantities with small but finite correlation times are approximated as white noise. Thus, simplified stochastic models constructed from atmospheric dynamical equations may assume Stratonovich calculus. However, if instead a stochastic model is indirectly estimated from observed discrete data, then the inferred drift will be the *sum* of the deterministic and the noise-induced drifts. In this case using the Itô framework may be preferable, where now $\mathbf{A}(\mathbf{x})$ represents not just the deterministic drift but rather this sum, or the "effective drift".

Equations for moments of $\mathbf{x}$ can be obtained by multiplying the Fokker-Planck equation (A.3) by powers of $\mathbf{x}$ and integrating over all $\mathbf{x}$. In particular, second moments of $\mathbf{x}$ are given by

$$\frac{d\langle \mathbf{x}\,\mathbf{x}^T\rangle}{dt} = \langle \mathbf{A}(\mathbf{x})\,\mathbf{x}^T\rangle + \langle \mathbf{x}\,\mathbf{A}^T(\mathbf{x})\rangle + \langle \mathbf{B}(\mathbf{x})\,\mathbf{B}^T(\mathbf{x})\rangle\,. \tag{A.4}$$

This equation is known as the fluctuation-dissipation relation (FDR) of the system (see e.g., Penland and Matrosova 1994).

In principle, the deterministic and stochastic parts of (A.3) can be determined from data by using their statistical definitions (Siegert et al. 1998; Friedrich et al. 2000; Gradišek et al.

2000; Sura and Barsugli 2002; Sura 2003; Sura and Gille 2003; Sura et al. 2006):

$$\mathbf{A}(\mathbf{x}) = \lim_{\Delta t \to 0} \frac{1}{\Delta t} \langle \mathbf{X}(t + \Delta t) - \mathbf{x} \rangle |_{\mathbf{X}(t)=\mathbf{x}} \tag{A.5}$$

$$\mathbf{B}(\mathbf{x})\mathbf{B}^T(\mathbf{x}) = \lim_{\Delta t \to 0} \frac{1}{\Delta t} \langle (\mathbf{X}(t + \Delta t) - \mathbf{x})(\mathbf{X}(t + \Delta t) - \mathbf{x})^T \rangle |_{\mathbf{X}(t)=\mathbf{x}} \tag{A.6}$$

where $\mathbf{X}(t+\Delta t)$ is a solution (a single stochastic realization) of the SDE (A.1) with the initial condition $\mathbf{X}(t) = \mathbf{x}$ at time t. The data define a state space representing every observed value of $\mathbf{x}$. The effective drift and stochastic diffusion are estimated by replacing the theoretical limit $\Delta t \to 0$ with a finite-difference approximation. In practice, estimating $\mathbf{B}(\mathbf{x})\mathbf{B}^T(\mathbf{x})$ from discretely sampled data is prone to error, because Taylor expansions of stochastic terms are proportional to $\sqrt{\Delta t}$ and not proportional to Δt as are the deterministic terms (e.g., Sura and Barsugli 2002; Sura 2003). Note that $\mathbf{B}(\mathbf{x})\mathbf{B}^T(\mathbf{x})$ rather than $\mathbf{B}(\mathbf{x})$ is estimated from data. In general it is impossible to find a unique expression for $\mathbf{B}(\mathbf{x})$ in the multivariate case (e.g., Monahan 2004).

When $\mathbf{A}$ and $\mathbf{B}$ are known, analytical solutions of the Fokker-Planck equation (A.3) for $p(\mathbf{x}, t)$ can only be found in limited cases (appendix B presents one such case). For more general cases, numerical methods must be used. To interpret the results of the Fokker-Planck equation, numerical integrations of the SDE (A.1) can also be performed.

References

Alexander, M. A., Blade, I., Newman, M., Lanzante, J. R., Lau, N.-C., and Scott, J. D., 2002: The atmospheric bridge: The influence of ENSO teleconnections on air-sea interaction over the global ocean. *J. Climate*, **14**, 2205–2231.

Alexander, M. A., and Penland, C., 1996: Variability in a mixed layer ocean model driven by stochastic atmospheric forcing. *J. Climate*, **9**, 2424–2442.

Alexander, M. A., and Scott, J. D., 1997: Surface flux variability over the North Pacific and North Atlantic oceans. *J. Climate*, **10**, 2963–2978.

Azzalini, A., 2005: *R package 'sn': The skew-normal and skew-t distribution (version 0.33).* Universit di Padova, Italia.

Azzalini, A., and Capitanio, A., 2003: Distributions generated by perturbations of symmetry with emphasis on a multivariate skew-t distribution. *J. R. Statist. Soc. B*, **65**, 367–389.

Barsugli, J. J., and Battisti, D. S., 1998: The basic effects of atmosphere-ocean thermal coupling on midlatitude variability. *J. Atmos. Sci.*, **55**, 477–493.

Chelton, D. B., Schlax, M. G., Freilich, M. H., and Milliff, R. F., 2004: Satellite measurements reveal persistent small-scale features in ocean winds. *Science*, **303**, 978–983.

Frankignoul, C., and Hasselmann, K., 1977: Stochastic climate models. Part II. Application to sea-surface temperature anomalies and thermocline variability. *Tellus*, **29**, 289–305.

Frankignoul, C., and Kestenare, E., 2002: The surface heat flux feedback. Part I: Estimates from observations in the Atlantic and the North Pacific. *Climate Dynamics*, **19**, 633–647.

Friedrich, R., Siegert, S., Peinke, J., Lück, S., Siefert, M., Lindemann, M., Raethjen, J., Deusch, G., and Pfister, G., 2000: Extracting model equations from experimental data. *Phys. Lett. A*, **271**, 217–222.

Gardiner, C. W., 2004: *Handbook of Stochastic Methods for Physics, Chemistry and the Natural Science, Third Edition*. Springer-Verlag, 415 pp.

Gille, S. T., 2005: Statistical characterization of zonal and meridonal ocean wind stress. *J. Atmos. Ocean. Tech.*, **22**, 1353–1372.

Gradišek, J., Siegert, S., Friedrich, R., and Grabec, I., 2000: Analysis of time series from stochastic processes. *Phys. Rev. E*, **62**, 3146–3155.

Hall, A., and Manabe, S., 1997: Can local linear stochastic theory explain sea surface temperature and salinity variability? *Climate Dyn.*, **13**, 167–180.

Hasselmann, K., 1976: Stochastic climate models. Part I. Theory. *Tellus*, **28**, 473–484.

Horsthemke, W., and Léfèver, R., 1984: *Noise-Induced Transitions: Theory and Applications in Physics, Chemistry, and Biology*. Springer-Verlag, 318 pp.

Jones, M. C., and Faddy, M. J., 2003: A skew extension of the *t*-distribution, with applications. *J. R. Statist. Soc. B*, **65**, 159–174.

Kloeden, P., and Platen, E., 1992: *Numerical Solution of Stochastic Differential Equations*. Springer-Verlag, 632 pp.

Kraus, E. B., and Businger, J. A., 1994: *Atmosphere-Ocean Interaction*. Oxford University Press, 362 pp.

Large, W. G., and Pond, S., 1982: Sensible and latent heat flux measurements over the ocean. *J. Phys. Oceanogr.*, **12**, 464–482.

Monahan, A. H., 2004: A simple model for the skewness of global sea-surface winds. *J. Atmos. Sci.*, **61**, 2037–2049.

Monahan, A. H., 2006a: The probability distributions of sea surface wind speeds Part I: Theory and SSM/I observations. *J. Climate*, **19**, 497–520.

Monahan, A. H., 2006b: The probability distributions of sea surface wind speeds Part II: Dataset intercomparison and seasonal variability. *J. Climate*, **19**, 521–534.

Mosedale, T. J., Stephenson, D. B., and Collins, M., 2005: Atlantic atmosphere-ocean interaction: A stochastic climate model-based diagnosis. *J. Climate*, **18**, 1086–1095.

Neelin, J. D., and Weng, W., 1999: Analytical prototypes for ocean-atmosphere interaction at midlatitudes. Part I: Coupled feedbacks as a sea surface dependent stochastic process. *J. Climate*, **12**, 2037–2049.

O'Neill, L. W., Chelton, D. B., and S K, E., 2003: Observations of sst-induced perturbations of the wind stress field of the Southern Ocean on seasonal time scales. *J. Climate*, **16**, 2340–2354.

Park, S., Deser, C., and Alexander, M. A., 2005: Estimation of the surface heat flux response to sea surface temperature anomalies over the global ocean. *J. Climate*, **18**, 4582–4599.

Paul, W., and Baschnagel, J., 1999: *Stochastic Processes: From Physics to Finance*. Springer-Verlag, 231 pp.

Peinke, J., Böttcher, F., and Barth, S., 2004: Anomalous statistics in turbulence, financial markets and other complex systems. *Ann. Phys.*, **13**, 450–460.

Penland, C., 1996: A stochastic model of Indo Pacific sea surface temperature anomalies. *Phys. D*, **98**, 543–558.

Penland, C., and Matrosova, L., 1994: A balance condition for stochastic numerical models with application to El Niño - the Southern Oscillation. *J. Climate*, **7**, 1352–1372.

R Development Core Team, 2004: *R: A language and environment for statistical computing*. R Foundation for Statistical Computing, Vienna, Austria, ISBN 3-900051-07-0.

Ronca, R. E., and Battisti, D. S., 1997: Anomalous sea surface temperatures and local air-sea energy exchange on intraannual timescale in the northeastern subtropical Pacific. *J. Climate*, **10**, 102–117.

Sardeshmukh, P., Penland, C., and Newman, M., 2001: Rossby waves in a fluctuating medium. P. Imkeller, and J.-S. von Storch, Eds., *Progress in Probability, Vol. 49: Stochastic Climate Models*, Birkhäuser Verlag, Basel.

Sardeshmukh, P. D., Penland, C., and Newman, M., 2003: Drift induced by multiplicative red noise with application to climate. *Europhysics Letters*, **63**, 498–504.

Siegert, S., Friedrich, R., and Peinke, J., 1998: Analysis of data sets of stochastic systems. *Phys. Lett. A*, **243**, 275–280.

Small, R. J., Xie, S.-P., and Hafner, J., 2005: Satellite observations of mesoscale ocean

features and copropagating atmospheric surface fields in the tropical belt. *J. Geophys. Res.*, **110**, C02021.

Sura, P., 2003: Stochastic analysis of Southern and Pacific Ocean sea surface winds. *J. Atmos. Sci.*, **60**, 654–666.

Sura, P., and Barsugli, J. J., 2002: A note on estimating drift and diffusion parameters from timeseries. *Phys. Lett. A*, **305**, 304–311.

Sura, P., and Gille, S. T., 2003: Interpreting wind-driven Southern Ocean variability in a stochastic framework. *J. Mar. Res.*, **61**, 313–334.

Sura, P., Newman, M., and Alexander, M. A., 2006: Daily to decadal sea surface temperature variability driven by state-dependent stochastic heat fluxes. *J. Phys. Oceanogr.*, **36**, 1940–1958.

Sura, P., Newman, M., Penland, C., and Sardeshmukh, P. D., 2005: Multiplicative noise and non-Gaussianity: A paradigm for atmospheric regimes? *J. Atmos. Sci.*, **62**, 1391–1409.

Xie, S.-P., 2004: Satellite observations of cool ocean-atmosphere interaction. *Bulletin of the American Meteorological Society*, **85**, 195–208.

Table captions

Table 1: The Ocean Weather Stations (OWSs) used for this study.

Figure captions

Figure 1: Solution of Eq. 7 (response with anomalous wind speeds; solid line) and Eq. 8 (response without anomalous wind speeds; dashed line) for $\overline{|\mathbf{U}|} \equiv 1$, $\sigma_{|\mathbf{U}|'} \equiv 0.5$, and $\delta T_o \equiv 1$. It can be seen that with anomalous wind speeds $\langle \delta T \rangle$ decays slightly slower than in the case with the mean wind only. That is, in this particular case (linear system with linear multiplicative noise) the stochastic forcing effectively reduces the damping of the system.

Figure 2: (a) Autocorrelation function and (b) PDF of wind speed anomalies (m/s) from observations at OWS P. Note that wind speed anomalies are almost uncorrelated after 2-3 days and that the distribution is almost Gaussian.

Figure 3: A schematic drawing to illustrate the physics/mathematics of our coupled model. We focus on the distinction between *air-sea interaction with mean wind only* (upper panel) and *air-sea interaction with mean and fluctuating winds* (lower panel). The physical set-ups are shown on the left hand sides of each panel, while the equivalent mathematical relations are depicted on the panel's right hand sides. In the case with only the mean wind the evolution of atmosphere-ocean temperatures, given by the deterministic drift matrix with parameters $-a, b, c, -d$, is visualized by the corresponding arrows: $-a$ damps the atmosphere, b is the

oceanic forcing of the atmosphere, c is the atmospheric forcing of the ocean, and $-d$ damps the ocean. Most importantly, note that in case were the heat flux is due to the mean and fluctuating winds the evolution of atmosphere-ocean temperatures, given by the effective drift matrix with parameters $-a + \frac{1}{2}\frac{(\sigma^M\beta)^2}{\gamma_a^2}, b - \frac{1}{2}\frac{(\sigma^M\beta)^2}{\gamma_a^2}, c - \frac{1}{2}\frac{(\sigma^M\beta)^2}{\gamma_a\gamma_o}, -d + \frac{1}{2}\frac{(\sigma^M\beta)^2}{\gamma_a\gamma_o}$, is altered by the noise-induced drift. The noise effectively decreases the absolute values of the damping and coupling parameters, altering the dynamics of air-sea interaction. See section 3 for a detailed discussion.

Figure 4: a-b) The effective drift $\mathbf{A}(\mathbf{x})$ estimated from AIRT and SST anomalies at OWS P, in units of K/d. $A1$ denotes the T'_a component (atmosphere) and $A2$ denotes the T'_o component (ocean) of the two-dimensional system. c) $(\mathbf{B}\mathbf{B}^T)_{11}$ element of the noise matrix $\mathbf{B}\mathbf{B}^T$, in units of $\mathrm{K}^2/\mathrm{d}^2$. See section 4.2 for details.

Figure 5: Autocorrelation functions (a) and PDFs (b) of the residual $\mathbf{r} \equiv \mathbf{T'}_{obs}(t+\Delta t) - \mathbf{T'}(t+\Delta t)$ for air temperature anomalies (thick solid lines) an sea surface temperature anomalies (dashed lines). Note that for both components the autocorrelation is close to zero after one time step of 1 day, and that the residuals are highly non-Gaussian (the thin sold line in (b) shows the related Gaussian distribution). See section 4.3 for details.

Figure 6: a) Modeled joint PDF anomalies (deviations from Gaussianity) of AIRT and SST anomalies with parameters for OWS P. b) Observed joint PDF anomalies (deviations from Gaussianity) of AIRT and SST anomalies at OWS P. Here AIRT and SST anomalies are normalized to have zero mean and unit standard deviation.

Figure 7: Spectra of modeled anomalous (a) AIRT and (b) SST variability without and with multiplicative noise for the first set of experiments (multiplicative noise turned off without accounting for lost variance). The spectra with pure additive noise are indicated by the dashed lines, and the spectra with multiplicative noise included are indicated by the solid lines.

Figure 8: Observed (left) and modeled (right) joint PDF anomalies (deviations from Gaussianity) of AIRT and SST anomalies at a) OWS K, and b) OWS N. Note that while the contour interval is the same in this plot and in Fig. 6, color shading is different for each station. Here AIRT and SST anomalies are normalized to have zero mean and unit standard deviation.

Table 1: The Ocean Weather Stations (OWSs) used for this study.

OWS	Location	Period
P	50°N, 145° W	1949–1981
N	30°N, 140° W	1946–1974
K	45°N, 16° W	1949–1975

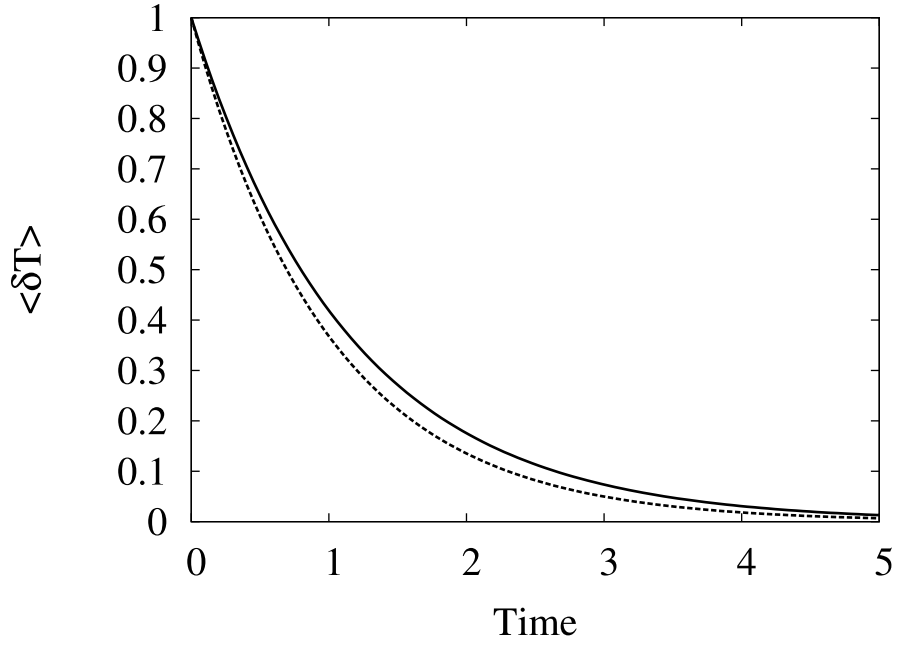

Figure 1: Solution of Eq. 7 (response with anomalous wind speeds; solid line) and Eq. 8 (response without anomalous wind speeds; dashed line) for $\overline{|\mathbf{U}|} \equiv 1$, $\sigma_{|\mathbf{U}|'} \equiv 0.5$, and $\delta T_o \equiv 1$. It can be seen that with anomalous wind speeds $\langle \delta T \rangle$ decays slightly slower than in the case with the mean wind only. That is, in this particular case (linear system with linear multiplicative noise) the stochastic forcing effectively reduces the damping of the system.

a)

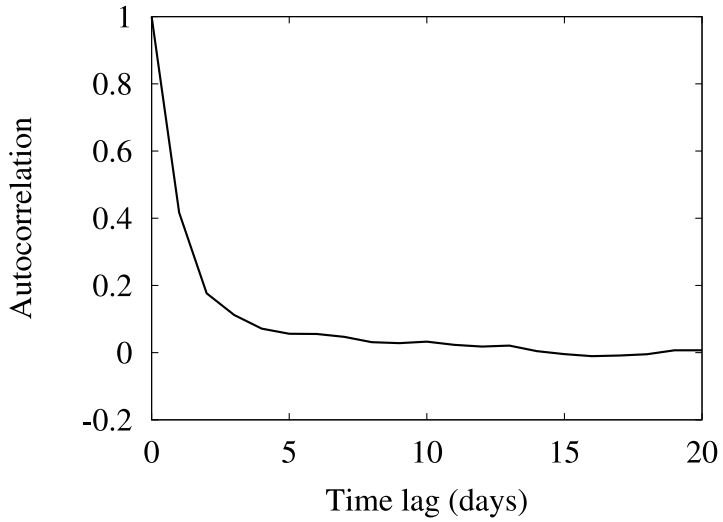

b)

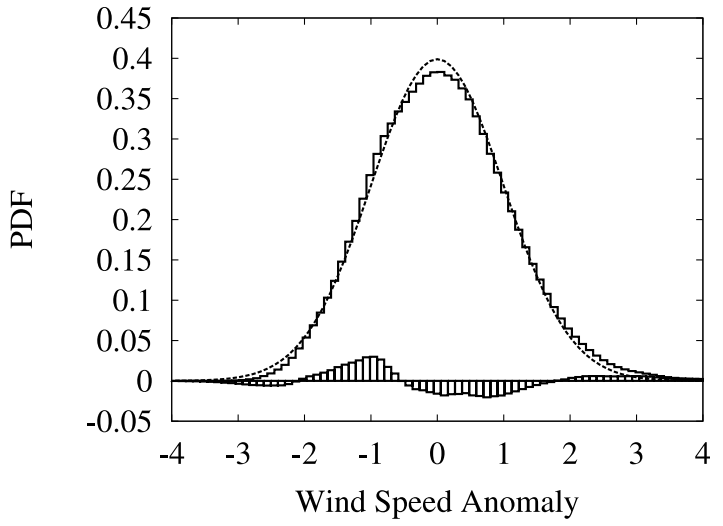

Figure 2: (a) Autocorrelation function and (b) PDF of wind speed anomalies (m/s) from observations at OWS P. Note that wind speed anomalies are almost uncorrelated after 2-3 days and that the distribution is almost Gaussian.

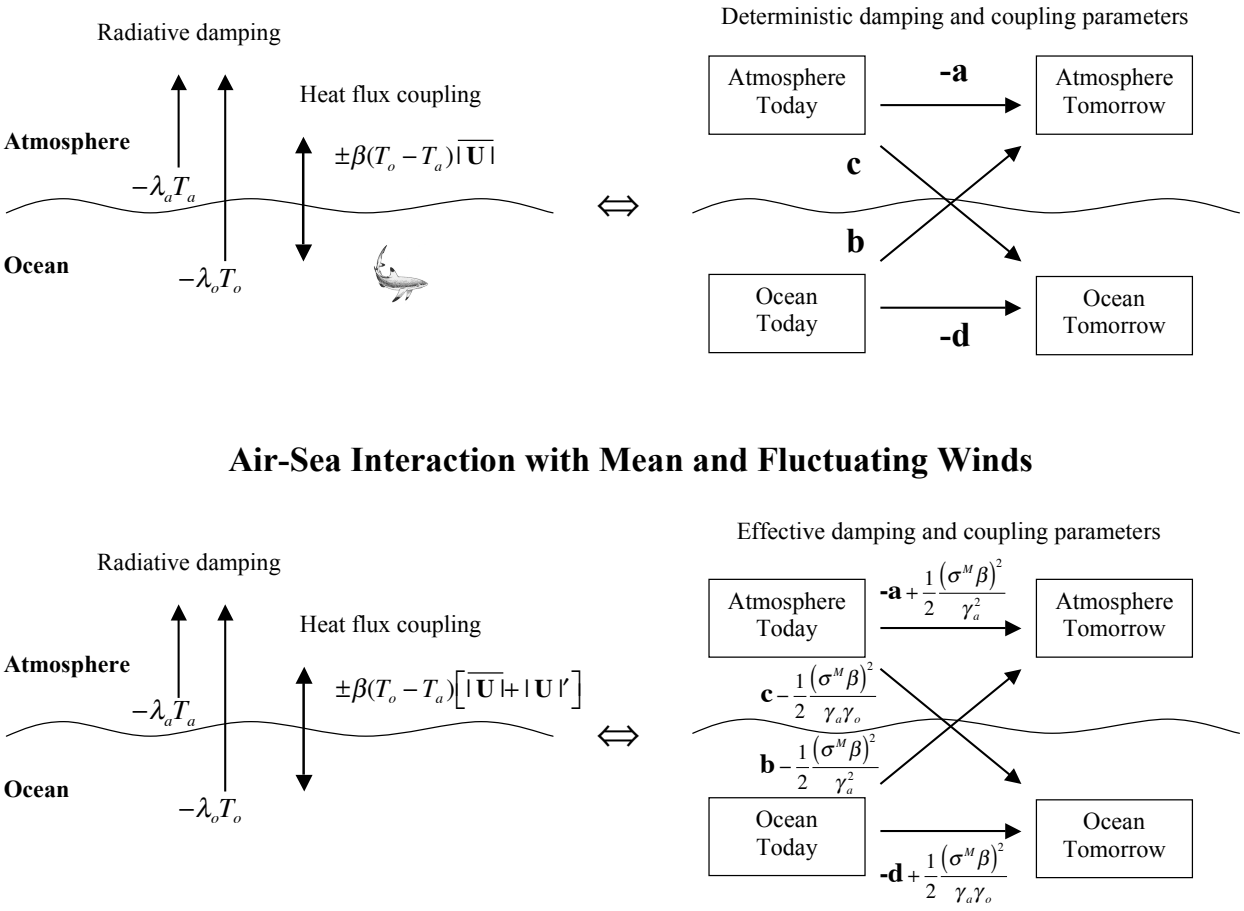

Figure 3: A schematic drawing to illustrate the physics/mathematics of our coupled model. We focus on the distinction between *air-sea interaction with mean wind only* (upper panel) and *air-sea interaction with mean and fluctuating winds* (lower panel). The physical set-ups are shown on the left hand sides of each panel, while the equivalent mathematical relations are depicted on the panel's right hand sides. In the case with only the mean wind the evolution of atmosphere-ocean temperatures, given by the deterministic drift matrix with parameters $-a, b, c, -d$, is visualized by the corresponding arrows: $-a$ damps the atmosphere, b is the oceanic forcing of the atmosphere, c is the atmospheric forcing of the ocean, and $-d$ damps the ocean. Most importantly, note that in case were the heat flux is due to the mean and fluctuating winds the evolution of atmosphere-ocean temperatures, given by the effective drift matrix with parameters $-a + \frac{1}{2}\frac{(\sigma^M\beta)^2}{\gamma_a^2}, b - \frac{1}{2}\frac{(\sigma^M\beta)^2}{\gamma_a^2}, c - \frac{1}{2}\frac{(\sigma^M\beta)^2}{\gamma_a\gamma_o}, -d + \frac{1}{2}\frac{(\sigma^M\beta)^2}{\gamma_a\gamma_o}$, is altered by the noise-induced drift. The noise effectively decreases the absolute values of the damping and coupling parameters, altering the dynamics of air-sea interaction. See section 3 for a detailed discussion.

a)

b)

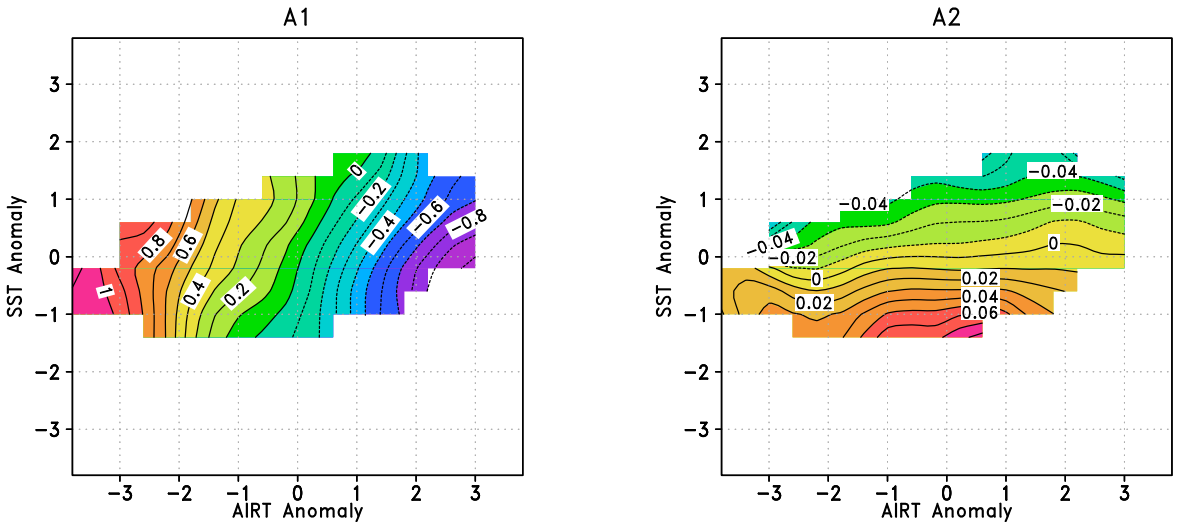

c)

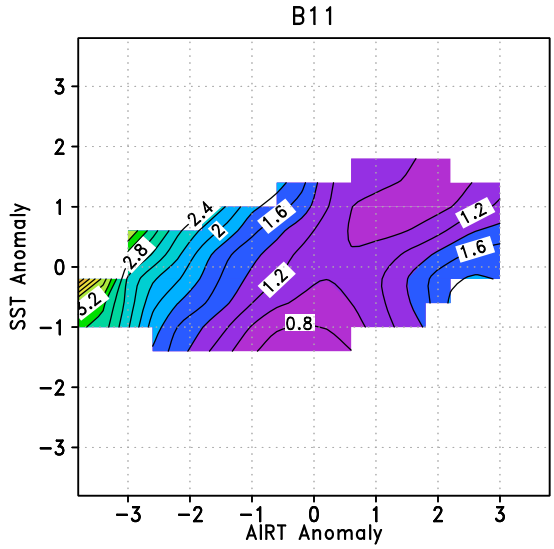

Figure 4: a-b) The effective drift $\mathbf{A}(\mathbf{x})$ estimated from AIRT and SST anomalies at OWS P, in units of K/d. $A1$ denotes the T'_a component (atmosphere) and $A2$ denotes the T'_o component (ocean) of the two-dimensional system. c) $(\mathbf{B}\mathbf{B}^T)_{11}$ element of the noise matrix $\mathbf{B}\mathbf{B}^T$, in units of $\mathrm{K}^2/\mathrm{d}^2$. See section 4.2 for details.

a)

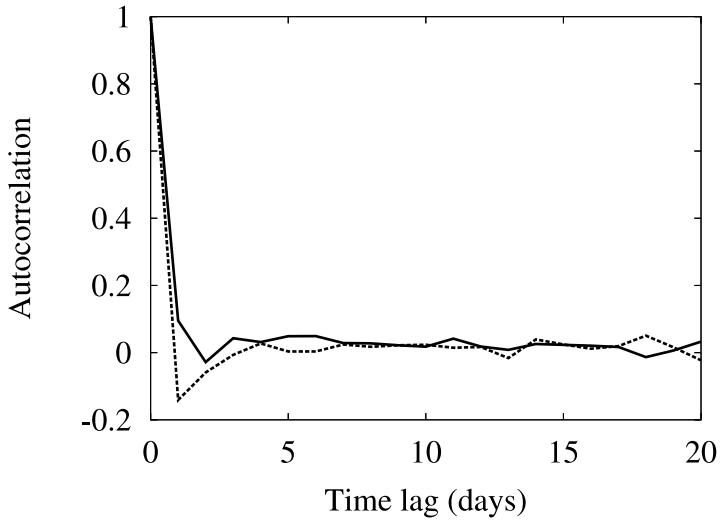

b)

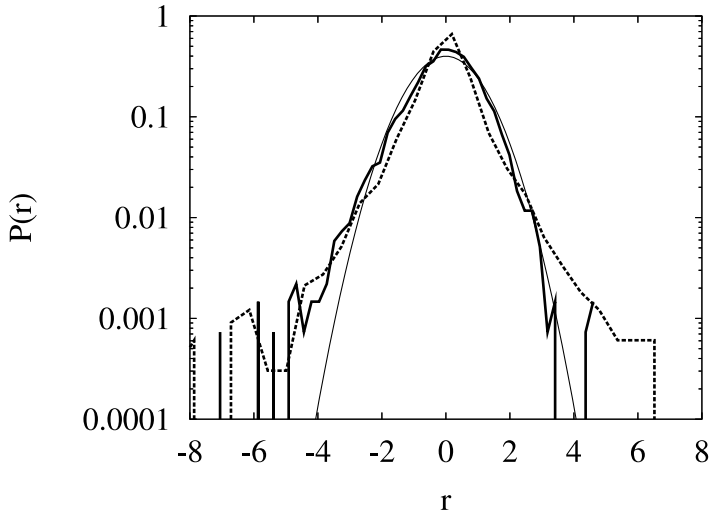

Figure 5: Autocorrelation functions (a) and PDFs (b) of the residual $\mathbf{r} \equiv \mathbf{T'}_{obs}(t+\Delta t) - \mathbf{T'}(t+\Delta t)$ for air temperature anomalies (thick solid lines) an sea surface temperature anomalies (dashed lines). Note that for both components the autocorrelation is close to zero after one time step of 1 day, and that the residuals are highly non-Gaussian (the thin sold line in (b) shows the related Gaussian distribution). See section 4.3 for details.

a)

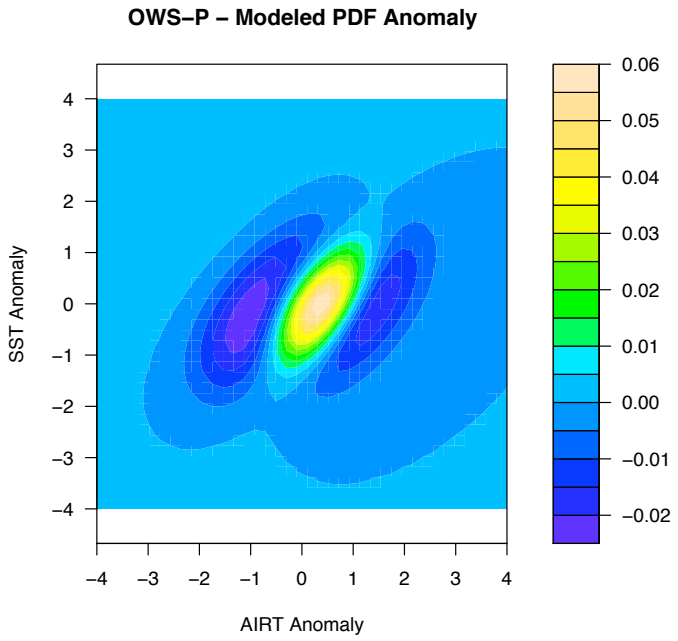

b)

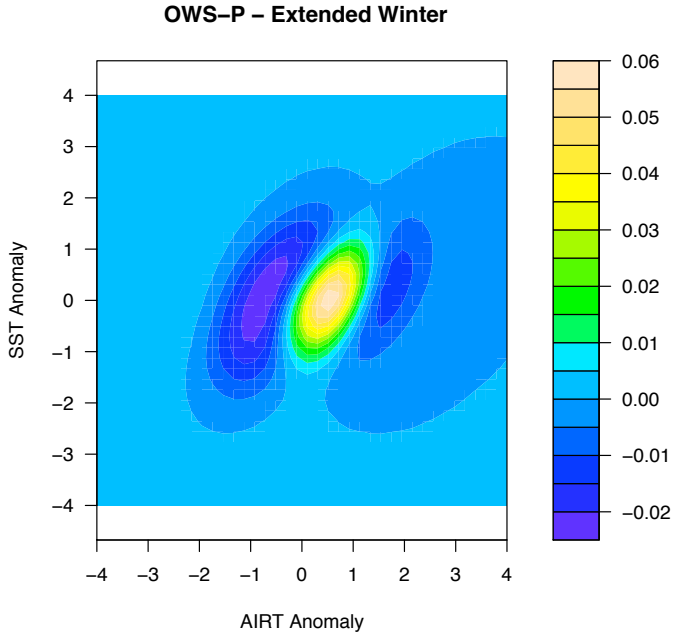

Figure 6: a) Modeled joint PDF anomalies (deviations from Gaussianity) of AIRT and SST anomalies with parameters for OWS P. b) Observed joint PDF anomalies (deviations from Gaussianity) of AIRT and SST anomalies at OWS P. Here AIRT and SST anomalies are normalized to have zero mean and unit standard deviation.

a)

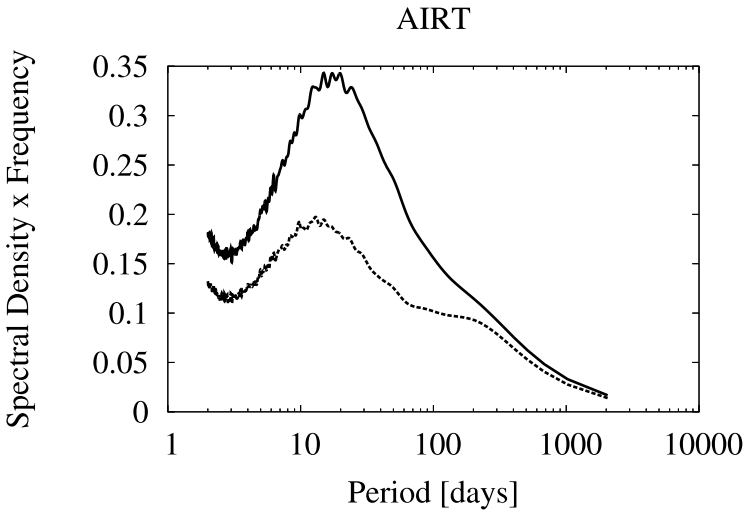

b)

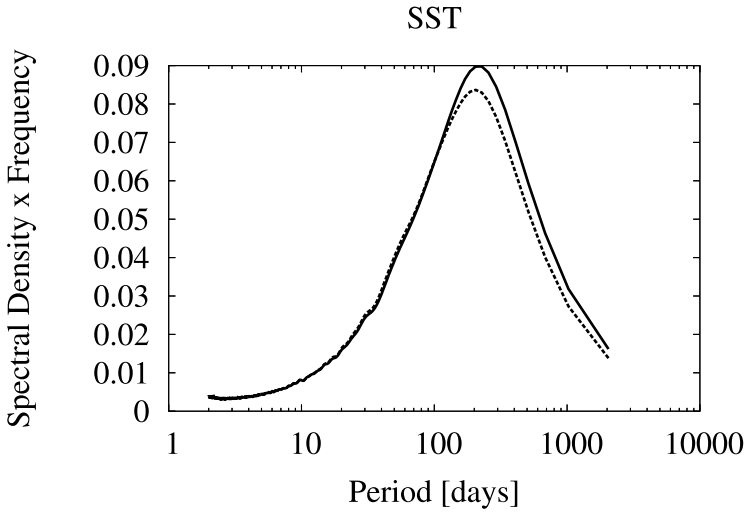

Figure 7: Spectra of modeled anomalous (a) AIRT and (b) SST variability without and with multiplicative noise for the first set of experiments (multiplicative noise turned off without accounting for lost variance). The spectra with pure additive noise are indicated by the dashed lines, and the spectra with multiplicative noise included are indicated by the solid lines.

b) OWS K (45° N, 16° W)

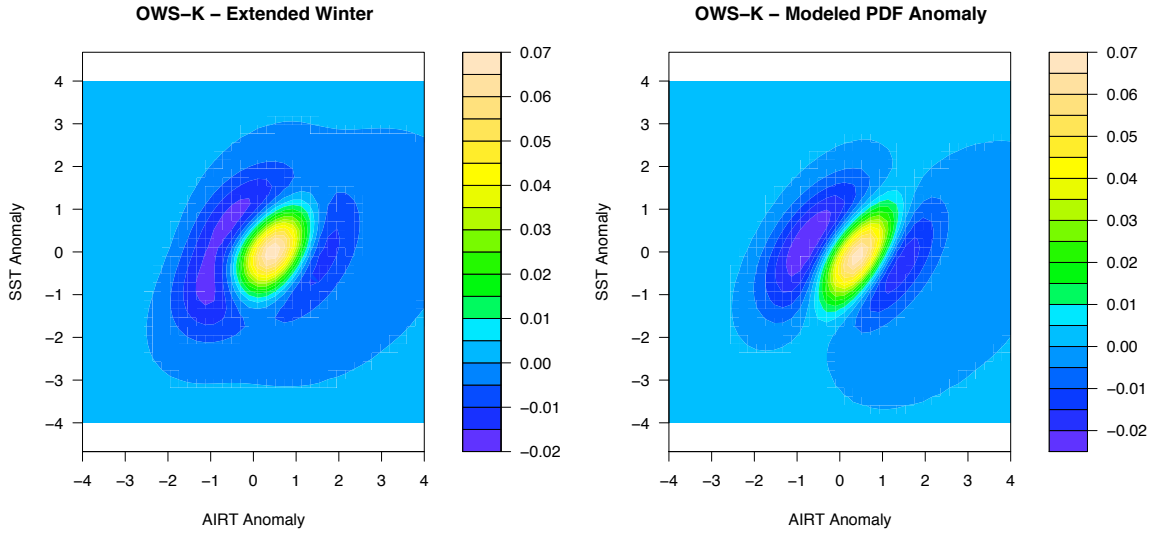

a) OWS N (30° N, 140° W)

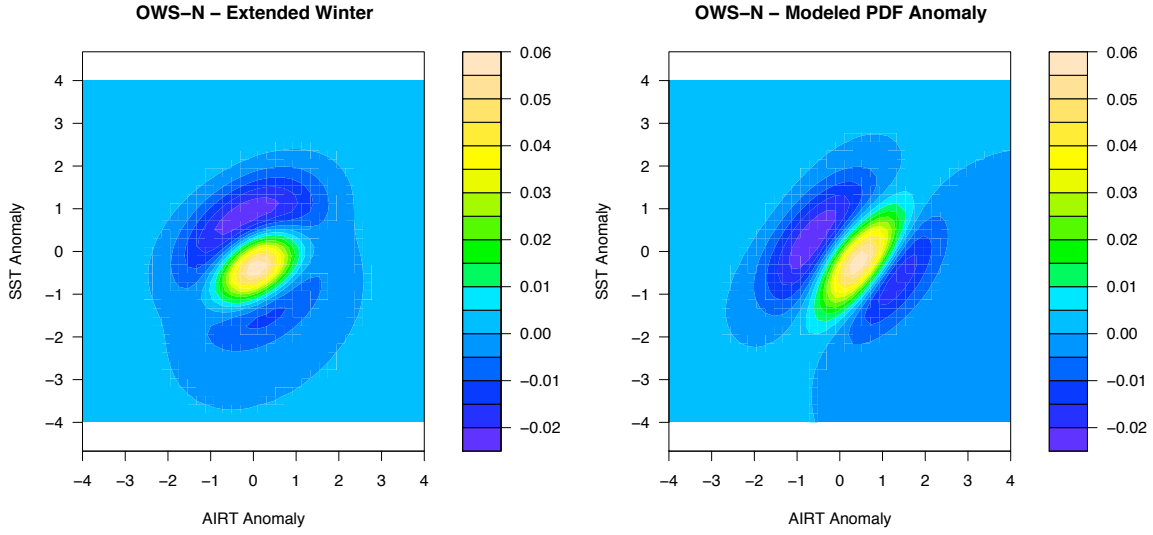

Figure 8: Observed (left) and modeled (right) joint PDF anomalies (deviations from Gaussianity) of AIRT and SST anomalies at a) OWS K, and b) OWS N. Note that while the contour interval is the same in this plot and in Fig. 6, color shading is different for each station. Here AIRT and SST anomalies are normalized to have zero mean and unit standard deviation.